

1 **Manuscript # acp-2019-778**

2
3 **Responses to Reviewer #1**

4
5
6 The study by Yang et al., attempted to quantify the contribution of major source
7 regions in the world towards aerosol loading in Europe. The study has certain flaws
8 which needs to be addressed before it can be accepted for publication at ACP.

9
10 We thank the reviewer for all the insightful comments. Below, please see our point-
11 by-point response (in blue) to the specific comments and suggestions and the
12 changes that have been made to the manuscript, in an effort to take into account all
13 the comments raised here.

14
15 Line 163: Any specific reason on why future DRF due to aerosols other than
16 sulphate was not estimated in this study for future. If not, I would suggest doing the
17 same.

18 **Response:**

19 Here in this study we focus both historical and future sulfate DRF rather than
20 other aerosol species. Aerosol DRF is defined in this study as the difference in clear-
21 sky radiative fluxes at the top of the atmosphere between two diagnostic calculations
22 in the radiative transfer scheme with and without specific aerosol species accounted,
23 respectively. Therefore, the DRF estimate requires additional calculations of
24 radiative fluxes. In default CAM5, less than 9 additional radiation calculations are
25 allowed. Since that the simulation was designed to output the DRF related to
26 emissions from Europe as well as few key source regions of the world that were
27 used in our previous studies, it was not feasible to separate all aerosol species for
28 the radiation diagnostic calculations. Considering that sulfate AOD accounts for the
29 largest portion (91%) of the decrease in total combustion AOD in Europe, the sulfate
30 DRF is calculated to roughly represent the DRF due to the total combustion AOD
31 change.

32 We have now added an explanation in the revised manuscript: "Rather than
33 sulfate, DRF of other aerosol species is not calculated in this study due to the
34 computational limitation considering multiple source regions. However, because
35 sulfate dominates the decrease in total combustion AOD in Europe shown below, the
36 sulfate DRF is calculated to roughly represent the DRF caused by the total
37 combustion AOD change."

38
39 Line 175: Why was nitrate and ammonium aerosols were not considered in this
40 study? I would suggest including nitrate at least.

41 **Response:**

42 The representation of nitrate and ammonium aerosols requires many additional
43 gas species and chemical/physical process treatments in models. Different from
44 regional air quality models, including complex chemistry and aerosol

thermodynamical equilibrium is less efficient for the long-term simulation in global aerosol-climate models. In the 3-mode version of modal aerosol model in CAM5, sulfate is partially neutralized by ammonium in the form of NH_4HSO_4 , so ammonium is effectively prescribed, but this model version cannot predict ammonium and nitrate. In the next version of CAM6, which will be released early next year, an advanced aerosol chemistry and microphysics module (called MOSAIC) will be implemented to treat tropospheric trace gas photochemistry, aerosol thermodynamics, kinetic gas-particle mass transfer and particle-phase chemistry, particularly, for nitrate aerosol. As a next step in our research plan, we will implement the tagging tool EAST to the new model version and analyze the source-receptor relationship of sulfate-nitrate-ammonium in future studies.

Line 218: I would strongly suggest to not compare the sum of BC, OC and sulphate with $\text{PM}_{2.5}$ from observations until aeolian dust, sea salt, nitrate and ammonium are presented/simulated. Additionally, I feel it is meaningless to compare the model AOD (without components like nitrate, ammonium) with AERONET.

Response:

Thanks for the suggestion. We have removed the $\text{PM}_{2.5}$ comparison in the manuscript and revised corresponding descriptions. For the comparison of model and observed AOD, although the sum of sulfate (or NH_4HSO_4 specifically), BC, POA, SOA, dust and sea salt cannot represent total aerosols in the real world, the comparison is still meaningful. The purpose here is to show the decreasing trend of AOD in Europe. Including nitrate aerosol in the simulation is unlikely to reverse the trend. So, we decide to keep the AERONET lines in the figure.

Line 220: Any specific reasons on why the model does not have the capability to simulate ammonium and nitrate aerosols.

Response:

Please see the responses above.

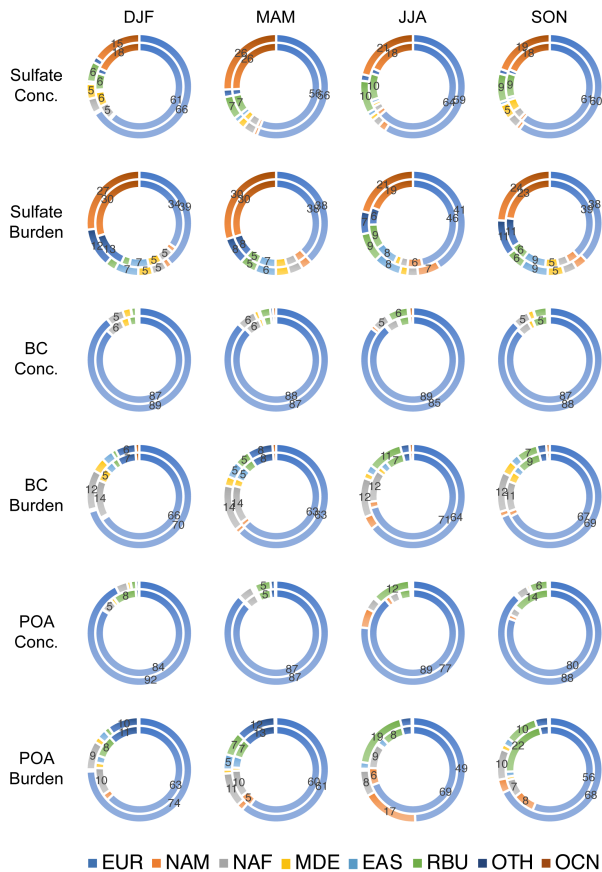
I strongly suggest the authors to include a section on seasonal source-receptor relationship for Europe supported by meteorological factors (like wind directions). I understand it is computationally expensive to carry out this for all the years considered in the study. However, performing seasonal analysis for a single representative year would suffice.

Response:

Thanks for the suggestion. We have now added the analysis of seasonal source-receptor relationship of aerosols in Europe and the role of meteorological factors based on an emission normalization method. Please see below:

“Source contributions to aerosols in Europe vary with season due to the seasonality of emissions and meteorology. In general, local sources have the largest contributions to both near-surface concentration and column burden of European aerosols in winter and smallest contributions in summer averaged over 2010–2018 (outer rings in Figure 7). With the contributions normalized by the ratio of seasonal

anthropogenic emission to annual mean for each source, the impact of emission seasonal variation on the source contributions can be removed (inner rings in Figure 7) (Yang et al., 2019). Without the influence of emission seasonality, local source contributions decrease in winter and increase in summer, indicating that it was the higher local anthropogenic emissions that result in the larger local source contributions to wintertime aerosols in Europe relative to other seasons. Sulfur sources over oceans account for one fourth to one third of European sulfate concentration and burden in spring likely due to the strong westerlies in this season that transport aerosols from the North Atlantic Ocean to the Europe. Source contributions from Russia-Belarus-Ukraine and North America to BC and POA in Europe show strong seasonal variabilities, which can be explained by the changes in biomass burning emissions considering its large seasonal variability."



103
104

Figure 6. Relative contributions (%) by emissions from major tagged source regions to near-surface concentrations (Conc.) and column burdens of December-January-February (DJF), March-April-May (MAM), June-July-August (JJA) and September-October-November (SON) mean sulfate, BC and POA over the Europe averaged over 2010–2018. Outer rings represent the modeled values and the relative contributions in inner rings is calculated based on absolute values normalized by the ratio of seasonal emission to annual mean. Values larger than 5% are marked.

Reference:

Yang, Y., Smith, S. J., Wang, H., Lou, S., and Rasch, P. J.: Impact of anthropogenic emission injection height uncertainty on global sulfur dioxide and aerosol distribution, *J. Geophys. Res.-Atmos.*, 124, 4812–4826. <https://doi.org/10.1029/2018JD030001>, 2019.

Responses to Reviewer #3

This study examined source apportionment of aerosols in Europe over 1980-2018 using the Community Atmosphere Model version 5 with an Explicit Aerosol Source Tagging technique (CAM5-EAST). They found that the near-surface total mass concentration of sulfate, black carbon and primary organic carbon had a 62% decrease and aerosols from foreign sources became increasingly important to air quality in Europe. They also estimated that contributions to the sulfate radiative forcing over Europe from both European local emissions and non-European emissions would decrease at a comparable rate in the next three decades. The CAM5-EAST model showed its advantage in simulating the aerosol source-receptor relationship within one model simulation. The topic is interesting and the manuscript is well organized. I suggest it published in the journal after addressing my minor comments below.

We thank the reviewer for all the insightful comments. Below, please see our point-by-point response (in blue) to the specific comments and suggestions and the changes that have been made to the manuscript, in an effort to take into account all the comments raised here.

The authors examined sulfate, black carbon and organic carbon aerosols in this study. Why did the author exclude other aerosols like nitrate in the simulation?

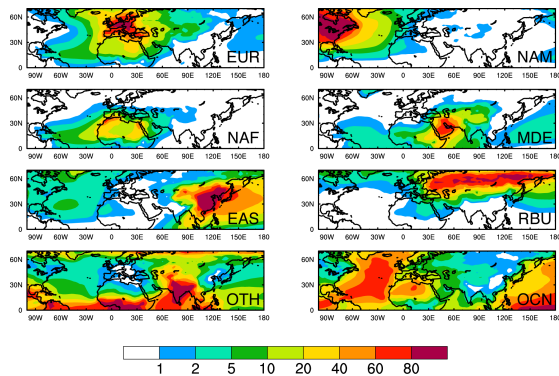
Response:

The representation of nitrate and ammonium aerosols requires many additional gas species and chemical/physical process treatments in models. Different from regional air quality models, including complex chemistry and aerosol thermodynamical equilibrium is less efficient for the long-term simulation in global aerosol-climate models. In the 3-mode version of modal aerosol model in CAM5, sulfate is partially neutralized by ammonium in the form of NH_4HSO_4 , so ammonium is effectively prescribed, but this model version cannot predict ammonium and nitrate. In the next version of CAM6, which will be released early next year, an advanced aerosol chemistry and microphysics module (called MOSAIC) will be implemented to treat tropospheric trace gas photochemistry, aerosol thermodynamics, kinetic gas-particle mass transfer and particle-phase chemistry, particularly, for nitrate aerosol. As a next step in our research plan, we will implement the tagging tool EAST to the new model version and analyze the source-receptor relationship of sulfate-nitrate-ammonium in future studies.

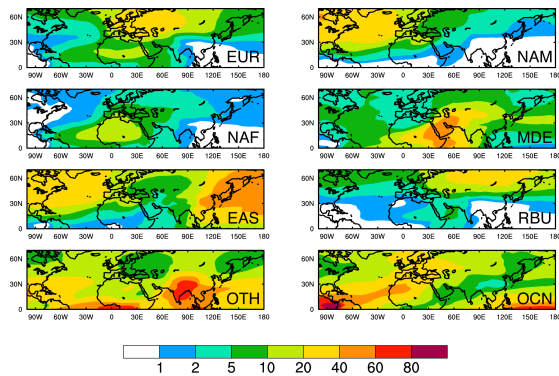
There seems a lot difference between the source attribution to near-surface concentration and column loading, as demonstrated in Figure 6. Thus, it would be more clear to directly show the transport pattern and source contributions near surface as well as those at higher altitude.

Response:

162 Thanks for the suggestion. We have now added the horizontal distribution of
 163 sulfate-BC-POA concentrations at the surface and 500 hPa, originating from the
 164 major tagged source regions, as shown below.
 165 “The transboundary and intercontinental transport of aerosols occur most
 166 frequently in the free troposphere rather than near the surface, as horizontal transport
 167 pathways at the surface and 500 hPa are indicated on the spatial distribution map of
 168 the relative contributions shown in Figures S2 and S3. This also leads to larger
 169 relative contributions from non-European sources to aerosol column burdens than to
 170 the near-surface concentrations.”
 171



172
 173 **Figure S2.** Relative contributions (%) to annual mean near-surface concentrations of
 174 sulfate-BC-POA from the major tagged source regions including Europe (EUR),
 175 North America (NAM), North Africa (NAF), the Middle East (MDE), East Asia (EAS),
 176 Russia-Belarus-Ukraine (RBU), Non-Arctic/Antarctic Ocean (OCN) and other (OTH)
 177 regions averaged over 2010–2018.
 178



179
 180 **Figure S3.** Relative contributions (%) to annual mean concentrations of sulfate-BC-
 181 POA at 500 hPa from the major tagged source regions including Europe (EUR),

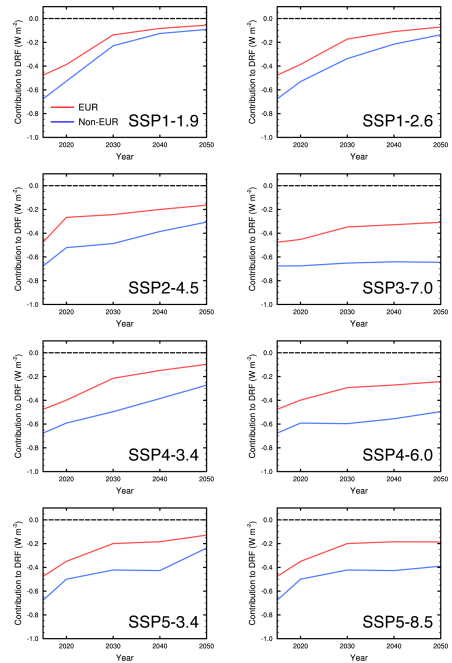
182 North America (NAM), North Africa (NAF), the Middle East (MDE), East Asia (EAS),
183 Russia-Belarus-Ukraine (RBU), Non-Arctic/Antarctic Ocean (OCN) and other (OTH)
184 regions averaged over 2010–2018.

186 In Figure 11, the areas represent minimum-to-maximum ranges. Is there a possibility
187 that one SSP scenario produces a minimum decrease in EUR contribution and a
188 maximum decrease in Non-EUR contribution?

189 Response:

190 We have now plotted the figure for each SSP scenario individually in Figure S4.
191 All SSPs show that non-European contributions change in a magnitude similar to
192 that of European local emissions.

193



194
195
196 **Figure S4.** Time series (2015–2050) of estimated annual mean sulfate DRF over
197 Europe contributed by European and non-European emissions from eight SSP
198 scenarios, including SSP1-1.9, SSP1-2.6, SSP2-4.5, SSP3-7.0, SSP4-3.4, SSP4-
199 6.0, SSP5-3.4, and SSP5-8.5. Future DRF of sulfate aerosol over Europe is
200 estimated by scaling historical mean (1980–2018) sulfate DRF using the ratio of
201 SSPs future SO₂ emissions to historical emissions assuming a linear response of
202 DRF to regional emissions.

203

What is the advantage of using CAM5-EAST rather than CAMx or CMAQ mentioned in the introduction section?

Response:

Influences of remote sources simulated in regional air quality models such as CAMx and CAMQ largely depend on the boundary conditions. They cannot tag and track the emissions outside the regional domain. As we discuss in the text, "However, due to the limitation in domain size of regional air quality models, contributions of intercontinental transport from sources outside the domain are difficult to be accounted." CAM5-EAST is a global model with aerosol tagging that has been used to examine the transboundary and transcontinental transport of aerosols in previous studies (Yang et al., 2018a,b).

The author analyzed annual averaged source contributions in this study. How is the source-receptor relationship in different seasons? Are they the same as the annual mean results?

Response:

Thanks for the suggestion. We have now added the analysis of seasonal source-receptor relationship of aerosols in Europe and the role of meteorological factors based on an emission normalization method. Please see below:

"Source contributions to aerosols in Europe vary with season due to the seasonality of emissions and meteorology. In general, local sources have the largest contributions to both near-surface concentration and column burden of European aerosols in winter and smallest contributions in summer averaged over 2010–2018 (outer rings in Figure 7). With the contributions normalized by the ratio of seasonal anthropogenic emission to annual mean for each source, the impact of emission seasonal variation on the source contributions can be removed (inner rings in Figure 7) (Yang et al., 2019). Without the influence of emission seasonality, local source contributions decrease in winter and increase in summer, indicating that it was the higher local anthropogenic emissions that result in the larger local source contributions to wintertime aerosols in Europe relative to other seasons. Sulfur sources over oceans account for one fourth to one third of European sulfate concentration and burden in spring likely due to the strong westerlies in this season that transport aerosols from the North Atlantic Ocean to the Europe. Source contributions from Russia-Belarus-Ukraine and North America to BC and POA in Europe show strong seasonal variabilities, which can be explained by the changes in biomass burning emissions considering its large seasonal variability."

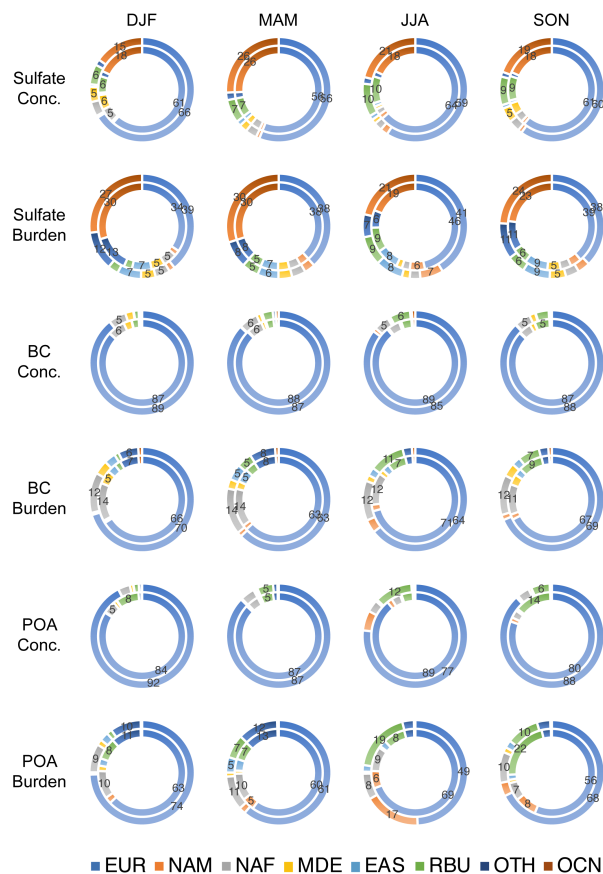


Figure 6. Relative contributions (%) by emissions from major tagged source regions to near-surface concentrations (Conc.) and column burdens of December-January-February (DJF), March-April-May (MAM), June-July-August (JJA) and September-October-November (SON) mean sulfate, BC and POA over the Europe averaged over 2010–2018. Outer rings represent the modeled values and the relative contributions in inner rings is calculated based on absolute values normalized by the ratio of seasonal emission to annual mean. Values larger than 5% are marked.

Page 11: What is temporal resolution of the observational data?

Response:

We have now added a description that “EMEP (European Monitoring and Evaluation Programme, <http://www.emep.int>) networks provide daily near-surface aerosol concentrations in Europe. The annual mean of daily observations is used to evaluate the model performance in this study.”

257
258
259
260
261
262
263
264
265
266
267
268
269
270
271
272
273
274
275
276
277
278

Fig.5: specify the abbreviations in the figure

Response:
Revised.

Reference:

Yang, Y., Wang, H., Smith, S. J., Zhang, R., Lou, S., Yu, H., Li, C., and Rasch, P. J.: Source apportionments of aerosols and their direct radiative forcing and long-term trends over continental United States, *Earth's Future*, 6, 793–808, <https://doi.org/10.1029/2018EF000859>, 2018a.

Yang, Y., Wang, H., Smith, S. J., Zhang, R., Lou, S., Qian, Y., Ma, P.-L., and Rasch, P. J.: Recent intensification of winter haze in China linked to foreign emissions and meteorology, *Sci. Rep.*, 8, 2107, <https://doi.org/10.1038/s41598-018-20437-7>, 2018b.

Yang, Y., Smith, S. J., Wang, H., Lou, S., and Rasch, P. J.: Impact of anthropogenic emission injection height uncertainty on global sulfur dioxide and aerosol distribution, *J. Geophys. Res.-Atmos.*, 124, 4812–4826. <https://doi.org/10.1029/2018JD030001>, 2019.

Trends and source apportionment of aerosols in Europe during
1980–2018

Yang Yang¹, Sijia Lou^{2*}, Hailong Wang³, Pinya Wang¹, Hong Liao¹

¹Jiangsu Key Laboratory of Atmospheric Environment Monitoring and Pollution
Control, Jiangsu Collaborative Innovation Center of Atmospheric Environment and
Equipment Technology, School of Environmental Science and Engineering, Nanjing
University of Information Science and Technology, Nanjing, Jiangsu, China

²School of Atmospheric Sciences, Nanjing University, Nanjing, Jiangsu, China

³Atmospheric Sciences and Global Change Division, Pacific Northwest National
Laboratory, Richland, Washington, USA

*Correspondence to lousijia@nju.edu.cn

300 **Abstract**

301 Aerosols have significantly affected health, environment and climate in Europe.
302 Aerosol concentrations have been declining since 1980s in Europe, mainly owing to
303 the reduction of local aerosol and precursor emissions. Emissions from other source
304 regions of the world, which have been changing rapidly as well, may also perturb the
305 historical and future trends of aerosols and change their radiative impact in Europe.
306 This study examines trends of aerosols in Europe during 1980–2018 and quantify
307 contributions from sixteen source regions using the Community Atmosphere Model
308 version 5 with an Explicit Aerosol Source Tagging technique (CAM5-EAST). The
309 simulated near-surface total mass concentration of sulfate, black carbon and primary
310 organic carbon had a 62% decrease during 1980–2018, of which the majority was
311 contributed by reductions of local emissions in Europe and 8%-9% was induced by
312 the decrease in emissions from Russia-Belarus-Ukraine. With the decreases in the
313 fractional contribution of local emissions, aerosols transported from other source
314 regions are increasingly important to air quality in Europe. During 1980–2018, the
315 decrease in sulfate loading leads to a warming effect of 2.0 W m^{-2} in Europe, with
316 12% coming from changes in non-European sources, especially from North America
317 and Russia-Belarus-Ukraine. According to the Shared Socioeconomic Pathways
318 (SSP) scenarios, contributions to the sulfate radiative forcing over Europe from both
319 European local emissions and non-European emissions would decrease at a
320 comparable rate in the next three decades, suggesting that future changes in non-

321 European emissions are as important as European emissions in causing possible
322 regional climate change associated with aerosols in Europe.

323

324

325

326 1. Introduction

327 Aerosols are main air pollutants that contribute to excess morbidity and
328 premature mortality through damaging cardiovascular and respiratory systems
329 (Lelieveld et al., 2019). They also have adverse effects on atmospheric visibility for
330 road and air traffic (Vautard et al., 2009). During the 1952 London Fog, high fatality
331 associated with extremely high level of aerosols caused thousands of premature
332 deaths (Bell and Davis, 2001), which resulted in a number of air quality legislations
333 for reducing air pollution in Europe (Brimblecombe et al., 2006).

334 Besides the health and environment effects, aerosols can significantly impact
335 regional and global climate through perturbing the Earth's radiation fluxes and
336 influencing cloud microphysics (Boucher et al., 2013). Globally, anthropogenic
337 aerosols exert a net cooling effect in the Earth system, which have dampened the
338 warming driven by greenhouse gases since the pre-industrial era. Due to a strong
339 surface albedo feedback over polar regions, per unit aerosol emission from western
340 Europe was reported to have the greatest cooling effect than other major source
341 regions of the globe (Persad and Caldeira, 2018), revealing the importance of
342 understanding aerosol variations in Europe.

343 Significant reductions in near-surface aerosol concentrations and aerosol optical
344 depth (AOD) have been observed in Europe during the last few decades from long-
345 term station measurements and satellite retrievals (de Meij et al., 2012; Tørseth et
346 al., 2012). The decrease in aerosols has been considered as a cause of the increase
347 in surface solar radiation over Europe since the 1980s (Wild, 2009), as well as the

348 contributor of the eastern European warming (Vautard et al., 2009), Arctic
349 amplification (Acosta Navarro et al., 2016), and the increased atmospheric visibility
350 over Europe (Stjern et al., 2011) during the past three decades.

351 The decrease in aerosols over Europe was mainly attributed to the continuous
352 reductions in European local anthropogenic emissions of aerosols and precursor
353 gases since the 1980s (Smith et al., 2011), as a result of legislations for improving
354 air quality. In addition to local emissions, aerosol levels can also be affected by
355 aerosol transport at continental scales (Zhang et al., 2017; Yang et al., 2018a).
356 Aerosol emissions in major economic regions of the world have been changing
357 rapidly during the past few decades owing to economic development and
358 environmental measures. North America has started reducing emissions since the
359 1980s, and emissions in Russia also showed decreasing trends after the dissolution
360 of the Soviet Union (Smith et al., 2011). In the meantime, aerosol emissions from
361 East Asia and South Asia have largely increased due to economic growth, although
362 emissions in China have been undergoing a remarkable reduction in the most recent
363 years, as a result of strict air quality regulations (Streets et al., 2000; Li et al., 2017).
364 It is important to understand the relative roles of local emissions and regional
365 transport in affecting long-term variation of aerosols in Europe from both air quality
366 and climate perspectives.

367 Source apportionment is useful for quantifying contributions to aerosols from
368 specific source regions and/or sectors, which is beneficial to the emission control
369 strategies. The traditional method of examining the source-receptor relationship in

370 aerosol models is to zero out or perturb a certain percent of emissions from a given
371 source region or sector in parallel sensitivity simulations along with a baseline
372 simulation, which has been used in many studies to examine source contributions of
373 particulate matter (PM) in Europe from different sectors (e.g., Sartelet et al., 2012;
374 Tagaris et al., 2015; Aksoyoglu et al., 2016). Recently, source region contributions to
375 European CO and O₃ levels, as well as global and regional aerosol radiative forcing,
376 were examined under the Hemispheric Transport of Air Pollution model experiment
377 phase 2 (HTAP2) protocol, in which sensitivity simulations were conducted with
378 anthropogenic emissions from different source regions reduced by 20% (Jonson et
379 al., 2018). This method suffers a large computational cost for the excessive model
380 simulations when estimating contributions from a large number of sources, and
381 contributions from all sources do not sum up to 100% of the total concentration in the
382 default simulation (Koo et al., 2009; Wang et al., 2014).

383 The explicit aerosol tagging method, which simultaneously tracks contributions
384 from many different sources, is a useful tool for assessing source-receptor
385 relationship of aerosols. This method has previous been adopted in regional air
386 quality models such as CAMx (the Comprehensive Air quality Model with
387 Extensions) and CMAQ (the Community Multi-scale Air Quality model). Using
388 regional air quality models with aerosol tagging, contributions from different source
389 sectors and local/regional sources to European PM and its health impact were
390 studied (Brandt et al., 2013; Skyllakou et al., 2014; Karamchandani et al., 2017).
391 However, due to the limitation in domain size of regional air quality models,

392 contributions of intercontinental transport from sources outside the domain are
393 difficult to be accounted.

394 Anthropogenic emissions of aerosols and their precursor gases from different
395 economic regions of the world have changed substantially during the past few
396 decades. Very few studies have examined the source apportionment of aerosols in
397 Europe from sources all over the changing world. In this study, source attributions of
398 concentrations, column burden, optical depth of aerosols in four major areas of
399 Europe from sixteen source regions of the globe over 1980–2018 are quantified,
400 which is facilitated by the explicit aerosol source tagging technique that were recently
401 implemented in a global aerosol-climate model (CAM5-EAST). This technique has
402 lately been used to examine source attribution of aerosol trends in China and U.S.
403 during 1980–2014 (Yang et al., 2018a,b). The source apportionment analysis is
404 extended to year 2018 using the Shared Socioeconomic Pathways (SSPs) scenario,
405 with a focus on Europe here.

406 The CAM5-EAST model, along with the aerosol source tagging technique, and
407 aerosol emissions are described in Sect. 2. Section 3 evaluates the model
408 performance in simulating aerosols in Europe. Section 4 show the analysis of
409 source-receptor relationships of aerosols in Europe in climatological mean. Source
410 contributions to long-term variations of European aerosols and their direct radiative
411 forcing (DRF) during 1980–2018, as well as future forcing prediction, are provided in
412 Sect. 5. Section 6 summarizes these results and conclusions.

413 2. Methods

Deleted: attrubutions

415 **2.1 Model Description and Experimental Setup**

416 The global aerosol-climate model CAM5 (Community Atmosphere Model version
417 5), which was developed as the atmospheric component of CESM (the Community
418 Earth System Model, Hurrell et al., 2013), is applied to simulate aerosols at a spatial
419 resolution of 1.9° latitude × 2.5° longitude and 30 vertical layers from the surface to
420 3.6 hPa. Aerosol species, including sulfate, black carbon (BC), primary organic
421 aerosol (POA), second organic aerosol (SOA), mineral dust and sea salt, can be
422 simulated in a modal aerosol module of CAM5. The three-mode aerosol module
423 (MAM3) configuration is chosen with the consideration of the computational
424 efficiency of long-term simulation. Details of the MAM3 aerosol representation in
425 CAM5 are described in Liu et al. (2012). On top of the default CAM5, some aerosol-
426 related scheme modifications are utilized to improve the model performance in the
427 aerosol convective transport and wet deposition (Wang et al., 2013).

428 A 40-year (1979–2018) historical AMIP-type (Atmospheric Model
429 Intercomparison Project) simulation has been performed, following CMIP6 (the
430 Coupled Model Intercomparison Project Phase 6) configurations and forcing
431 conditions. Time-varying sea surface temperatures, sea ice concentrations, solar
432 insolation, greenhouse gas concentrations and aerosol emissions are prescribed in
433 the simulation. To better reproduce large-scale circulation patterns for aerosol
434 transport in the model, wind fields are nudged to the MERRA-2 (Modern Era
435 Retrospective-Analysis for Research and Applications Version 2) reanalysis (Ronald
436 Gelaro et al., 2017).

437 Aerosol DRF is defined in this study as the difference in clear-sky radiative fluxes
438 at the top of the atmosphere between two [diagnostic](#) calculations in the radiative
439 transfer scheme with and without specific [aerosol species](#) accounted, respectively.
440 Historical variation of [sulfate](#) DRF due to anthropogenic emissions from Europe and
441 outside Europe are quantified in this study. [Rather than sulfate, DRF of other aerosol](#)
442 [species is not calculated in this study due to the computational limitation considering](#)
443 [multiple source regions. However, because sulfate dominates the decrease in total](#)
444 [combustion AOD in Europe shown below, the sulfate DRF is calculated to roughly](#)
445 [represent the DRF caused by the total combustion AOD change.](#) Future DRF of
446 sulfate aerosol over Europe is also estimated through scaling historical mean (1980–
447 2018) sulfate DRF by the ratio of SSPs future SO₂ emissions to historical emissions
448 assuming a linear response of DRF to AOD and regional emissions. This DRF
449 prediction method has been used to estimate the East Asian contribution to sulfate
450 DRF in U.S. in 2030s (Yang et al., 2018a).

451 2.2 Aerosol Source Tagging Technique

452 The Explicit Aerosol Source Tagging (EAST) technique, which was recently
453 implemented in CAM5 (Wang et al., 2014; Yang et al., 2017a, b), is used to examine
454 the long-term source apportionment of aerosols in Europe. Unlike the traditional
455 back-trajectory and emission perturbation methods, EAST has the identical physical,
456 chemical and dynamical processes considered independently for aerosol species
457 (defined as new tracers) emitted from each of the tagged source region and/or sector
458 in the simulation. Sulfate, BC, POA and SOA from pre-defined sources can be

Deleted: parallel

Deleted: aerosols

Deleted: aerosol

462 explicitly tracked, from emission to deposition, in one CAM5-EAST simulation. Due
463 to the computational constraint and potentially large model bias from the simplified
464 SOA treatment (Yang et al., 2018a; Lou et al., 2019), we focus on sulfate, BC and
465 POA in this study but quantify the potential impact of SOA on the aerosol variation.

466 The global aerosol and precursor emissions are decomposed into sixteen source
467 regions defined in the HTAP2 protocol, including Europe (EUR), North America
468 (NAM), Central America (CAM), South America (SAM), North Africa (NAF), South
469 Africa (SAF), the Middle East (MDE), Southeast Asia (SEA), Central Asia (CAS),
470 South Asia (SAS), East Asia (EAS), Russia-Belarus-Ukraine (RBU), Pacific-
471 Australia-New Zealand (PAN), the Arctic (ARC), Antarctic (ANT), and Non-
472 Arctic/Antarctic Ocean (OCN) (Figure 1). Note that sources from marine and volcanic
473 eruptions are included in OCN. The focused receptor region in this study is Europe,
474 which is further divided into Northwestern Europe (NWE or NW Europe),
475 Southwestern Europe (SWE or SW Europe), Eastern Europe (EAE or E. Europe)
476 and Greece-Turkey-Cyprus (GTC) based on the finer source region selection in
477 HTAP2.

478 **2.3 Aerosol and Precursor Emissions**

479 Following the CMIP6-AMIP protocol, historical anthropogenic (Hoesly et al.,
480 2018) and biomass burning (van Marle et al., 2017) emissions of aerosol and
481 precursor gases are used over 1979–2014. For the remaining four years (2015–
482 2018), emissions are interpolated from the SSP2-4.5 forcing scenario, in which
483 aerosol pathways are not as extreme as other SSPs and have been used in many

model intercomparison projects for CMIP6 (O'Neill et al., 2016). Figure S1 shows the spatial distribution and time series of anthropogenic emissions of SO₂ (precursor gas of sulfate aerosol), BC and POA from Europe over 1980–2018. High emissions are located over E. Europe and NW Europe, from which the emissions of SO₂, BC and POA were reduced by 84–93%, 43–62% and 28–36%, respectively, in 2014–2018 relative to 1980–1984. Although SW Europe had a relatively low total amount of emissions compared to E. Europe and NW Europe, it had significant reductions in SO₂ and BC emissions, 91% and 55%, respectively. Over GTC region, SO₂ and BC emissions were increased by 49% and 48%, respectively. Considering the sub-regions as a whole, SO₂, BC and POA emissions from Europe have decreased by 12.57 Tg yr⁻¹ (83%), 0.22 Tg yr⁻¹ (46%) and 0.30 Tg yr⁻¹ (24%) in 2014–2018 compared to 1980–1984 (Table 1). Historical changes in emissions from other source regions can be found in Hoesly et al. (2018) and Yang et al. (2018b).

3 Model Evaluation

EMEP (European Monitoring and Evaluation Programme, <http://www.emep.int>) networks provide daily near-surface aerosol concentrations in Europe. The annual mean of daily observations is used to evaluate the model performance in this study. Compared to the observational data from EMEP networks during 2010–2014, CAM5-EAST can well reproduce the spatial distribution and magnitude of aerosol components with normalized mean biases (NMB) of -14%~ -23% and correlation coefficients (R) in a range of 0.43~0.62 for sulfate, BC and organic carbon (OC, derived from POA and SOA from the model results) (Figures 2).

Deleted: 2

Deleted: (European Monitoring and Evaluation Programme, <http://www.emep.int>)

Deleted: 3

Deleted: a, b, c

Deleted: The model underestimates the mean concentration of PM_{2.5} (sum of sulfate, BC, POA and SOA) by 59% relative to EMEP data (Figure 3d), although the spatial distribution has a strong correlation with the observations (R=0.72). It is partially because the model version used in this study does not have the ability to simulate nitrate and ammonium aerosols, which can be the major constituents of PM_{2.5} in some regions, and the fine-mode mineral dust and sea salt is not included in the estimated PM_{2.5} either.

Figure 3 shows the time series of annual mean near-surface sulfate, BC, and OC concentrations averaged over EMEP sites in Europe and the corresponding model values during 1993–2018. Variations in near-surface sulfate concentrations are consistent between the model and observations, with R values higher than 0.9. The observed variations of BC and OC concentrations in Europe are represented in the simulation, with R values of 0.52 and 0.65, respectively. However, the observed high values of BC and OC concentrations are not captured by the model, probably because very few data were available before 2010 and, therefore, any difference between model and observation cannot be smoothed out through the spatial average. This is also indicated by the large spatial variation of BC and OC concentrations before 2010. Nevertheless, the modeled concentrations are still within the range of observations. Note that the number of sites used for the spatial average in Figure 3 is different from year to year and thus the variation or trend here does not represent that over a sub-region or the entire Europe.

The modeled AOD is evaluated against the AERONET (Aerosol Robotic Network, <https://aeronet.gsfc.nasa.gov>) data in Figure 8. Both the modeled and observed AOD show decreasing trends during 2001–2018. The model underestimates AOD in all four sub-regions of Europe probably due to the lack of nitrate aerosol. The variations of AOD in Western Europe (combined NW and SW Europe) are well predicted with R values of about 0.75, but the model barely reproduces the AOD variations in E. Europe and the GTC region ($R < 0.5$). The difference of the interannual variation in AOD between the model simulation and

Deleted: 4

Deleted: and PM_{2.5}

Deleted: and PM_{2.5}

Deleted: PM_{2.5} concentrations are lower in the model simulation than observations in almost all years, confirming the role of the missing aerosol species in contributing to PM_{2.5} as discussed above.

Deleted: 4

Deleted: and ammonium

Deleted: s

553 observation can be caused by many factors such as aerosol emissions, aerosol
554 parameterizations in model, aerosol mixing state, inaccurate meteorological fields
555 from reanalysis data, and biases in measurements. However, identifying the
556 contribution of each factor to the difference is beyond the scope of this paper.

557 **4. Source Apportionment of Aerosols in Europe**

558 Based on the tagging technique in CAM5-EAST, near-surface concentrations of
559 total sulfate-BC-POA can be attributed to emissions within and outside Europe, as
560 shown in Figures [4a](#) and [4b](#), and the relative contributions in percentage are given in
561 Figures [4c](#) and [4d](#). Averaged over 2010–2018, due to the relatively high local
562 emissions, annual mean sulfate-BC-POA concentrations contributed by European
563 emissions show peak values of $4 \mu\text{g m}^{-3}$ in E. Europe. The slight increase in SO_2
564 emission from the GTC region (Figure [S1](#)), which is opposite to the decreases in the
565 other three sub-regions of Europe, also leads to high concentrations in GTC, with 2–
566 $4 \mu\text{g m}^{-3}$ contributed by European emissions. Due to the atmospheric transport from
567 surrounding regions including North Africa, the Middle East and [Russia-Belarus-](#)
568 [Ukraine](#), non-European emissions account for $0.5\text{--}1 \mu\text{g m}^{-3}$ over SW Europe, E.
569 Europe and GTC area. Overall, European local emissions are the dominant sources
570 of sulfate-BC-POA near-surface concentrations in Europe with contributions larger
571 than 80% (60%) in central areas (most of Europe). Non-European emissions are
572 responsible for 30–50% of the near-surface concentrations near the coastal areas
573 and boundaries of the Europe that are easily influenced by aerosol regional
574 transport.

Deleted: 5a

Deleted: 5b

Deleted: 5c

Deleted: 5d

Deleted: 2

Deleted: RBU

581 Figure 5 illustrates the source contributions in percentage of emissions from
582 different regions of the globe to near-surface aerosol concentrations and column
583 burdens over the four sub-regions of Europe averaged over 2010–2018. Different
584 aerosols have fairly different local/remote source attributions depending on the local
585 to remote emission ratio and transport efficiency. European emissions explain 54%–
586 68% of near-surface sulfate concentrations over the four sub-regions of Europe, with
587 the largest local contribution in E. Europe due to the relatively high emission rate.

Deleted: 6

588 The emissions from Europe dominate BC and POA concentrations in Europe with
589 contributions in the range of 78%–95% and 58%–78%, respectively. The impact of
590 local emissions on near-surface sulfate concentration is smaller than BC and POA.
591 This is partially due to the less efficient gas scavenging than particles and the
592 additional SO₂-to-sulfate conversion process that increases the atmospheric
593 residence time of sulfur. On the other hand, the higher initial injection height of SO₂
594 emissions from some sources (e.g., industrial sector and power plants) facilitates the
595 lifting of SO₂ and sulfate aerosol into the free atmosphere and, therefore, favors the
596 long-range transport (Yang et al., 2019). The efficient reduction in local SO₂
597 emissions in Europe also caused the lower influences of local emissions on sulfate
598 concentrations in recent years.

Deleted: from

599 Anthropogenic emissions over oceans (e.g., international shipping) and natural
600 emissions of oceanic dimethyl sulfide (DMS) and volcanic activities together account
601 for 16%–28% of near-surface sulfate concentrations in the four sub-regions of
602 Europe. About 10% of sulfate and 5%–10% of BC and POA in E. Europe and GTC

605 come from [Russia-Belarus-Ukraine](#) emissions. North Africa contributes to 7% of
606 sulfate, 17% of BC and 24% of POA over SW Europe. The contributions of
607 emissions, from the Middle East, to aerosol concentrations in GTC are between 5%
608 and 10%.

Deleted: RBU

609 [The transboundary and intercontinental transport of aerosols occur most](#)
610 [frequently in the free troposphere rather than near the surface, as horizontal transport](#)
611 [pathways at the surface and 500 hPa are indicated on the spatial distribution map of](#)
612 [the relative contributions shown in Figures S2 and S3. This also leads to larger](#)
613 [relative contributions from non-European sources to aerosol column burdens than to](#)
614 [the near-surface concentrations](#), (Figure 5). The European emissions only contribute
615 32%–47% of column burden of sulfate, 57%–75% of BC and 51%–71% of POA over
616 the four sub-regions of Europe. Over NW Europe and SW Europe, about 10%–15%
617 of the sulfate burden is from East Asia and [Russia-Belarus-Ukraine](#), respectively.

Deleted: The transboundary and intercontinental transport of aerosols occur most frequently in the free troposphere rather than near the surface, leading to larger relative contributions from non-European sources to aerosol column burdens than to the near-surface concentrations...

Deleted: 6

Deleted: RBU

618 Sources in North Africa are responsible for 27% and 14% of BC and 19% and 11%
619 of POA burden over SW Europe and GTC, respectively. Emissions from North
620 America account for 15% and 10% POA burden over NW Europe and SW Europe,
621 respectively. Emissions from [Russia-Belarus-Ukraine](#) explain 12% and 19% of POA
622 burden over E. Europe and GTC, respectively. Since near-surface aerosol
623 concentrations directly affect air quality and column burden is more relevant to
624 radiative impact, the differences of relative contributions between near-surface
625 concentrations and column burden highlight the possible roles of non-local emissions
626 in either air quality or energy balance over Europe.

Deleted: RBU

[Source contributions to aerosols in Europe vary with season due to the seasonality of emissions and meteorology. In general, local sources have the largest contributions to both near-surface concentration and column burden of European aerosols in winter and smallest contributions in summer averaged over 2010–2018 \(outer rings in Figure 6\). With the contributions normalized by the ratio of seasonal anthropogenic emission to annual mean for each source, the impact of emission seasonal variation on the source contributions can be removed \(inner rings in Figure 6\) \(Yang et al., 2019\). Without the influence of emission seasonality, local source contributions decrease in winter and increase in summer, indicating that it was the higher local anthropogenic emissions that result in the larger local source contributions to wintertime aerosols in Europe relative to other seasons. Sulfur sources over oceans account for one fourth to one third of European sulfate concentration and burden in spring likely due to the strong westerlies in this season that transport aerosols from the North Atlantic Ocean to the Europe. Source contributions from Russia-Belarus-Ukraine and North America to BC and POA in Europe show strong seasonal variabilities, which can be explained by the changes in biomass burning emissions considering its large seasonal variability.](#)

5. Source Apportionment of Long-term Trends

Total sulfate-BC-POA concentrations decreased during 1980–2018 over all of the four sub-regions of Europe (Figure 7), since that near-surface aerosol concentrations in Europe are dominated by its local emissions and the European anthropogenic emissions have significantly decreased during this time period.

659 Averaged over the entire Europe, near-surface concentrations of sulfate, BC and
660 POA decreased by 70%, 43% and 23%, respectively, between 1980–1984 and
661 2014–2018, which is consistent with the decreases in local emissions (Table 1). The
662 total sulfate-BC-POA concentrations decreased by 62%. With SOA included, this
663 value does not have a substantial change (from 62% to 59%) and the decreasing
664 trends in the four sub-regions of the Europe are not largely affected either. The
665 column burden of sulfate, BC, POA and the sum of these three decreased by 60%,
666 28%, 4% and 55%, respectively, which is less than the decrease in corresponding
667 near-surface concentration. It is because non-local emissions have larger influences
668 at high altitudes than at the surface, which partly dampened the contribution of near-
669 surface aerosol decrease (induced by reductions in location emissions) to the
670 column integration.

671 The decrease in European local emissions explains 93% of the reduced
672 concentration and 91% of the reduced burden in Europe between the first and last
673 five-year period of 1980–2018, while 8%–9% is contributed by the reduction in
674 emissions from [Russia-Belarus-Ukraine](#) (Table 2). The decrease in emissions from
675 North America also explains 10% of the reduced column burden of sulfate-BC-POA
676 in Europe from 1980–1984 to 2014–2018. Along with the decreases in local emission
677 contributions to near-surface sulfate-BC-POA concentrations in Europe, the fraction
678 of non-European emission contributions increased from 10%–30% to 30%–50%
679 during 1980–2018 (Figure 7), indicating that aerosols from foreign emissions through
680 long-range transport have become increasingly important to air quality in Europe.

Deleted: RBU

682 Regulations for further improvement of air quality in Europe in the near future need
683 to take changes in non-European emissions into account.

684 Similar to the declining trend in column burden, simulated total AOD also
685 decreased from 0.12–0.16 to 0.06–0.08 in NW Europe and SW Europe and from
686 0.19–0.21 to 0.09–0.13 in E. Europe and GTC region during the past four decades
687 (Figure 8). Sulfate AOD accounts for the largest portion of total combustion AOD
688 (sum of sulfate, BC, POA and SOA) over the four sub-regions of Europe. The
689 combustion AOD has decreased by 0.065 from 1980–1984 to 2014–2018 (Table 1),
690 with 0.059 (91%) contributed by the decrease in sulfate AOD. Therefore, we focus
691 on sulfate aerosol when examining the decadal changes in AOD and DRF in Europe
692 below.

693 The decreased sulfate AOD can also be decomposed into different contributions
694 from individual source regions in CAM5-EAST. European local emissions contribute
695 to 89% of the decrease, followed by 9% and 7% attributed to changes in emissions
696 from [Russia-Belarus-Ukraine](#) and North America, respectively, with the residual
697 offset by other source regions (Table 2). Over the last four decades, model simulated
698 sulfate AOD decreased at a rate of 0.017, 0.017, 0.026 and 0.012 decade⁻¹,
699 respectively, over NW Europe, SW Europe, E. Europe and GTC. Decreases in
700 European local SO₂ emissions result in 78% of the sulfate AOD decreases over GTC
701 and about 90% over the other three sub-regions (Figure 9). For the remote sources,
702 emission changes in North America explain 5%–10% of the European sulfate AOD
703 decrease, while [Russia-Belarus-Ukraine](#) sources contribute 29% of the sulfate AOD

Deleted: RBU

Deleted: RBU

706 decrease over GTC and 6%–8% over NW Europe and E. Europe, indicating a
707 possible warming enhancement effect of changes in emissions from North America
708 and [Russia-Belarus-Ukraine](#).

Deleted: RBU

709 Averaged over 1980–2018, sulfate imposed a cooling effect over Europe with the
710 maximum negative DRF at the top of the atmosphere (TOA) exceeding -3 W m^{-2} in
711 E. Europe (Figure 10). Compared to 1980–1984, the magnitude of sulfate DRF
712 decreased in 2014–2018, leading to a $1\text{--}3 \text{ W m}^{-2}$ warming mainly in E. Europe. The
713 warming effect mostly came from local SO_2 emission reduction, while non-European
714 emission changes only contributed less than 0.4 W m^{-2} over most regions of the
715 Europe. Considering Europe as a whole, the decrease in sulfate DRF caused a
716 warming effect of 2.0 W m^{-2} , with 88% and 12% coming from reductions European
717 local emissions and changes in non-European emissions, respectively (Tables 1 and
718 2).

719 Future changes in sulfate DRF associated with European and non-European
720 emissions based on eight SSP scenarios are also estimated and shown in Figure 11_
721 [and Figure S4 gives the estimate for each SSP scenario](#). Sulfate DRF contributed by
722 both European and non-European emissions would decrease in the near future but
723 has large variabilities between different SSPs. The sulfate DRF (cooling) over
724 Europe contributed from European local emissions shows a decrease from -0.48 W
725 m^{-2} in year 2015 to -0.18 ($-0.08 \sim -0.33$) W m^{-2} in year 2030 and -0.14 ($-0.05 \sim -0.29$)
726 W m^{-2} in year 2050. Unlike their contributions to the historical (1980–2018) change,
727 non-European emissions have an increasingly significant impact on the future sulfate

DRF changes in Europe. The contributions of non-European emissions decrease from -0.68 W m^{-2} in year 2015 to -0.39 ($-0.13 \sim -0.64$) W m^{-2} in year 2030 and -0.26 ($-0.08 \sim -0.63$) W m^{-2} in year 2050, with the changes in a magnitude similar to that of European local emissions. It suggests that future changes in non-European emissions are as important as European emissions to radiative balance and associated regional climate change in Europe.

6. Conclusions

Using a global aerosol-climate model with an explicit aerosol source tagging technique (CAM5-EAST), we examine the long-term trends and source apportionment of aerosols in Europe over 1980–2018 from sixteen source regions covering the globe in this study. CAM5-EAST can well capture the spatial distribution and temporal variation of aerosol species in Europe during this time period.

Averaged over 2010–2018, European emissions account for 54%–68%, 78%–95% and 58%–78% of near-surface sulfate, BC, and POA concentrations over Europe, respectively. [Russia-Belarus-Ukraine](#) emissions explain 10% of sulfate in E. Europe and GTC. North Africa contributes to 17% of BC and 24% of POA over SW Europe. Anthropogenic emissions over oceans (e.g., from international shipping) and natural emissions from marine and volcanic activities together account for 16%–28% of sulfate near-surface concentrations in Europe. European emissions only account for 32%–47%, 57%–75% and 51%–71% of column burden of sulfate, BC and POA, respectively, in Europe, with the rest contributed by emissions from East Asia, [Russia-Belarus-Ukraine](#), North Africa and North America. [Source contributions of](#)

Deleted: -

Deleted: , although it underestimates $\text{PM}_{2.5}$ concentration and total AOD due in part to the lack of representation of nitrate and ammonium aerosols in the model...

Deleted: RBU

Deleted: RBU

758 [aerosols in Europe vary with seasons driven by the seasonality of emissions and](#)
759 [meteorology.](#)

760 Compared to 1980–1984, simulated total sulfate-BC-POA near-surface
761 concentration and column burden over 2014–2018 had a decrease of 62% and 55%,
762 respectively, the majority of which was contributed by reductions in European local
763 emissions. The decrease in emissions from [Russia-Belarus-Ukraine](#) contributed 8%–
764 9% of the near-surface concentration decrease, while the decrease in emissions
765 from North America accounted for 10% of the reduced column burden. With the large
766 decrease in local emission contribution, aerosols from foreign sources became
767 increasingly important to air quality in Europe. The decrease in sulfate led to a 2.0 W
768 m² warming in Europe, with 12% coming from changes in non-European emissions,
769 especially in North America and [Russia-Belarus-Ukraine](#). Based on the SSP
770 scenarios and the assumed relationship between DRF and emissions, we estimated
771 that sulfate DRF over Europe contributed from European emissions and non-
772 European emissions would decrease at a comparable rate in the near future. This
773 suggests that future changes in non-European emissions are as important as
774 European emissions in affecting regional climate change associated with aerosols in
775 Europe. It should also be noted that the model currently does not have the ability to
776 simulate nitrate and ammonium aerosols and, therefore, the conclusions may not
777 hold with all aerosols.

778

779

Deleted: RBU

Deleted: RBU

782 ***Data availability.***

783 The default CAM5 model is publicly available at
784 <http://www.cesm.ucar.edu/models/cesm1.2/> (last access: 16 August 2019). Our
785 CAM5-EAST model code and results can be made available through the National
786 Energy Research Scientific Computing Center (NERSC) servers upon request.

787

788 ***Competing interests.***

789 The authors declare that they have no conflict of interest.

790

791 ***Author contribution.***

792 YY, SL, and HW designed the research; YY performed the model simulations; YY,
793 and SL analyzed the data. All the authors discussed the results and wrote the paper.

794

795 ***Acknowledgments.***

796 This research was support by the National Natural Science Foundation of China
797 under grant 41975159, the U.S. Department of Energy (DOE), Office of Science,
798 Biological and Environmental Research as part of the Earth and Environmental
799 System Modeling program, Jiangsu Specially Appointed Professor Project, and the
800 Startup Fund for Talent at NUIST under Grant 2019r047. The Pacific Northwest
801 National Laboratory is operated for DOE by Battelle Memorial Institute under
802 contract DE-AC05-76RLO1830. The National Energy Research Scientific Computing
803 Center (NERSC) provided computational support.

References

- Acosta Navarro, J. C., Varma, V., Riipinen, I., Seland, Ø., Kirkevåg, A., Struthers, Iversen, H., T., Hansson, H.-C., and Ekman, A. M. L.: Amplification of Arctic warming by past air pollution reductions in Europe, *Nat. Geosci.*, 9, 277–281, <https://doi.org/10.1038/ngeo2673>, 2016.
- Aksoyoglu, S., Baltensperger, U., and Prévôt, A. S. H.: Contribution of ship emissions to the concentration and deposition of air pollutants in Europe, *Atmos. Chem. Phys.*, 16, 1895–1906, doi:10.5194/acp-16-1895-2016, 2016.
- Bell, M. L., and Davis, D. L.: Reassessment of the Lethal London Fog of 1952: Novel Indicators of Acute and Chronic Consequences of Acute Exposure to Air Pollution, *Environ. Health Perspect.*, 109, 389–394, <https://doi.org/10.1289/ehp.01109s3389>, 2001.
- Boucher, O., Randall, D., Artaxo, P., Bretherton, C., Feingold, G., Forster, P., Kerminen, V. M., Kondo, Y., Liao, H., Lohmann, U., Rasch, P., Satheesh, S. K., Sherwood, S., Stevens, B., and Zhang, X. Y.: Clouds and Aerosols, in: *Climate Change 2013: The Physical Science Basis, Contribution of Working Group I to the Fifth Assessment Report of the Intergovernmental Panel on Climate Change*, edited by: Stocker, T. F., Qin, D., Plattner, G.-K., Tignor, M., Allen, S. K., Boschung, J., Nauels, A., Xia, Y., Bex, V., Midgley, P. M. Cambridge University Press, Cambridge, United Kingdom and New York, NY, USA, 571–658, 2013.
- Brandt, J., Silver, J. D., Christensen, J. H., Andersen, M. S., Bønløkke, J. H., Sigsgaard, T., Geels, C., Gross, A., Hansen, A. B., Hansen, K. M., Hedegaard, G. B., Kaas, E., and Frohn, L. M.: Contribution from the ten major emission sectors in Europe and Denmark to the health-cost externalities of air pollution using the EVA model system – an integrated modelling approach, *Atmos. Chem. Phys.*, 13, 7725–7746, <https://doi.org/10.5194/acp-13-7725-2013>, 2013.
- Brimblecombe, P.: The Clean Air Act after 50 Years, *Weather*, 61, 311–314, <https://doi.org/10.1256/wea.127.06>, 2006.
- de Meij, A., Pozzer, A., and Lelieveld, J.: Trend analysis in aerosol optical depths and pollutant emission estimates between 2000 and 2009, *Atmos. Environ.*, 51, 75–85, <https://doi.org/10.1016/j.atmosenv.2012.01.059>, 2012.
- Gelaro, R., McCarty, W., Suárez, M. J., Todling, R., Molod, A., Takacs, L., Randles, C. A., Darmenov, A., Bosilovich, M. G., Reichle, R., Wargan, K., Coy, L., Cullather, R., Draper, C., Akella, S., Buchard, V., Conaty, A., da Silva, A. M., Gu, W., Kim, G.-K., Koster, R., Lucchesi, R., Merkova, D., Nielsen, J. E., Partyka, G., Pawson, S., Putman, W., Rienecker, M., Schubert, S. D., Sienkiewicz, M., and

Zhao, B.: The Modern-Era Retrospective Analysis for Research and
 Applications, Version 2 (MERRA-2), *J. Climate*, 30, 5419–5454,
<https://doi.org/10.1175/JCLI-D-16-0758.1>, 2017.

Hoesly, R. M., Smith, S. J., Feng, L., Klimont, Z., Janssens-Maenhout, G., Pitkanen,
 T., Seibert, J. J., Vu, L., Andres, R. J., Bolt, R. M., Bond, T. C., Dawidowski, L.,
 Kholod, N., Kurokawa, J.-I., Li, M., Liu, L., Lu, Z., Moura, M. C. P., O'Rourke, P.
 R., and Zhang, Q.: Historical (1750–2014) anthropogenic emissions of reactive
 gases and aerosols from the Community Emissions Data System (CEDS),
Geosci. Model Dev., 11, 369–408, <https://doi.org/10.5194/gmd-11-369-2018>,
 2018.

Hurrell, J. W., Holland, M. M., Gent, P. R., Ghan, S., Kay, J. E., Kushner, P. J.,
 Lamarque, J. F., Large, W. G., Lawrence, D., Lindsay, K., Lipscomb, W. H.,
 Long, M. C., Mahowald, N., Marsh, D. R., Neale, R. B., Rasch, P., Vavrus, S.,
 Vertenstein, M., Bader, D., Collins, W. D., Hack, J. J., Kiehl, J., and Marshall, S.:
 The Community Earth System Model A Framework for Collaborative Research,
B. Am. Meteorol. Soc., 94, 1339–1360, <https://doi.org/10.1175/BAMS-D-12-00121.1>, 2013.

Jonson, J. E., Schulz, M., Emmons, L., Flemming, J., Henze, D., Sudo, K., Tronstad
 Lund, M., Lin, M., Benedictow, A., Koffi, B., Dentener, F., Keating, T., Kivi, R.,
 and Davila, Y.: The effects of intercontinental emission sources on European air
 pollution levels, *Atmos. Chem. Phys.*, 18, 13655–13672,
<https://doi.org/10.5194/acp-18-13655-2018>, 2018.

Karamchandani, P., Long, Y., Pirovano, G., Balzarini, A., and Yarwood, G.: Source-
 sector contributions to European ozone and fine PM in 2010 using AQMEII
 modeling data, *Atmos. Chem. Phys.*, 17, 5643–5664, <https://doi.org/10.5194/acp-17-5643-2017>, 2017.

Koo, B., Wilson, G. M., Morris, R. E., Dunker, A. M., and Yarwood, G.: Comparison
 of source apportionment and sensitivity analysis in a particulate matter air quality
 model, *Environ. Sci. Technol.*, 43, 6669–6675,
<https://doi.org/10.1021/es9008129>, 2009.

Lelieveld, J., Klingmüller, K., Pozzer, A., Burnett, R. T., Haines, A. and Ramanathan,
 V.: Effects of fossil fuel and total anthropogenic emission removal on public
 health and climate, *Proc. Natl. Acad. Sci.*, 116, 7192–7197,
<https://doi.org/10.1073/pnas.1819989116>, 2019.

Li, C., McLinden, C., Fioletov, V., Krotkov, N., Carn, S., Joiner, J., Streets, D., He,
 H., Ren, X., Li, Z., and Dickerson, R. R.: India Is Overtaking China as the

World's Largest Emitter of Anthropogenic Sulfur Dioxide, *Scientific Reports*, 7, 14304, <https://doi.org/10.1038/s41598-017-14639-8>, 2017.

O'Neill, B. C., Tebaldi, C., van Vuuren, D. P., Eyring, V., Friedlingstein, P., Hurtt, G., Knutti, R., Kriegler, E., Lamarque, J.-F., Lowe, J., Meehl, G. A., Moss, R., Riahi, K., and Sanderson, B. M.: The Scenario Model Intercomparison Project (ScenarioMIP) for CMIP6, *Geosci. Model Dev.*, 9, 3461–3482, <https://doi.org/10.5194/gmd-9-3461-2016>, 2016.

Persad, G. G., and Caldeira, K.: Divergent global - scale temperature effects from identical aerosols emitted in different regions, *Nat. Commun.*, 9, 3289. <https://doi.org/10.1038/s41467-018-05838-6>, 2018.

Riahi, K., van Vuuren, D. P., Kriegler, E., Edmonds, J., O'Neill, B. C., Fujimori, S., Bauer, N., Calvin, K., Dellink, R., Fricko, O., Lutz, W., Popp, A., Crespo Cuaresma, J., KC, S., Leimbach, M., Jiang, L., Kram, T., Rao, S., Emmerling, J., Ebi, K., Hasegawa, T., Havlik, P., Humenöder, F., Aleluia Da Silva, L., Smith, S., Stehfest, E., Bosetti, V., Eom, J., Gernaat, D., Ma- sui, T., Rogelj, J., Streffer, J., Drouet, L., Krey, V., Luderer, G., Harmsen, M., Takahashi, K., Baumstark, L., Doelman, J., Kainuma, M., Klimont, Z., Marangoni, G., Lotze-Campen, H., Obersteiner, M., Tabeau, A., and Tavoni, M.: The Shared Socioeconomic Pathways and their energy, land use, and greenhouse gas emissions implications: An Overview, *Global Environ. Chang.*, 42, 153–168, <https://doi.org/10.1016/j.gloenvcha.2016.05.009>, 2017.

Sartelet, K. N., Couvidat, F., Seigneur, C., and Roustan, Y.: Impact of biogenic emissions on air quality over Europe and North America, *Atmos. Environ.*, 53, 131–141, <https://doi.org/10.1016/j.atmosenv.2011.10.046>, 2012.

Skyllakou, K., Murphy, B. N., Megaritis, A. G., Fountoukis, C., and Pandis, S. N.: Contributions of local and regional sources to fine PM in the megacity of Paris, *Atmos. Chem. Phys.*, 14, 2343–2352, <https://doi.org/10.5194/acp-14-2343-2014>, 2014.

Smith, S. J., van Aardenne, J., Klimont, Z., Andres, R. J., Volke, A., and Delgado Arias, S.: Anthropogenic sulfur dioxide emissions: 1850–2005, *Atmos. Chem. Phys.*, 11, 1101–1116, <https://doi.org/10.5194/acp-11-1101-2011>, 2011.

Stjern, C. W., Samset, B. H., Myhre, G., Bian, H., Chin, M., Davila, Y., Dentener, F., Emmons, L., Flemming, J., Haslerud, A. S., Henze, D., Jonson, J. E., Kucsera, T., Lund, M. T., Schulz, M., Sudo, K., Takemura, T., and Tilmes, S.: Global and regional radiative forcing from 20 % reductions in BC, OC and SO₄ – an HTAP2 multi-model study, *Atmos. Chem. Phys.*, 16, 13579–13599, <https://doi.org/10.5194/acp-16-13579-2016>, 2016.

935
936 Stjern, C. W., Stohl, A., and Kristjánsson, J. E.: Have aerosols affected trends in
937 visibility and precipitation in Europe?, *J. Geophys. Res.*, 116, D02212,
938 <https://doi.org/10.1029/2010JD014603>, 2011.
939
940 Streets, D. G., Tsai, N. Y., Akimoto, H., and Oka, K.: Sulfur dioxide emissions in Asia
941 in the period 1985–1997, *Atmos. Environ.*, 34, 4413–4424,
942 [https://doi.org/10.1016/S1352-2310\(00\)00187-4](https://doi.org/10.1016/S1352-2310(00)00187-4), 2000.
943
944 Tagaris, E., Sotiropoulou, R., Gounaris, N., Andronopoulos, S., and Vlachogiannis,
945 D.: Effect of the Standard Nomenclature for Air Pollution (SNAP) categories on
946 air quality over Europe, *Atmosphere*, 6, 1119, doi:10.3390/atmos6081119, 2015.
947
948 Tørseth, K., Aas, W., Breivik, K., Fjæraa, A. M., Fiebig, M., Hjellbrekke, A. G., Lund
949 Myhre, C., Solberg, S., and Yttri, K. E.: Introduction to the European Monitoring
950 and Evaluation Programme (EMEP) and observed atmospheric composition
951 change during 1972–2009, *Atmos. Chem. Phys.*, 12, 5447–5481,
952 <https://doi.org/10.5194/acp-12-5447-2012>, 2012.
953
954 van Marle, M. J. E., Kloster, S., Magi, B. I., Marlon, J. R., Daniau, A.-L., Field, R. D.,
955 Arneth, A., Forrest, M., Hantson, S., Kehrwald, N. M., Knorr, W., Lasslop, G., Li,
956 F., Mangeon, S., Yue, C., Kaiser, J. W., and van der Werf, G. R.: Historic global
957 biomass burning emissions for CMIP6 (BB4CMIP) based on merging satellite
958 observations with proxies and fire models (1750–2015), *Geosci. Model Dev.*, 10,
959 3329–3357, <https://doi.org/10.5194/gmd-10-3329-2017>, 2017.
960
961 Vautard, R., Yiou, P., and Oldenborgh, G.: Decline of fog, mist and haze in Europe
962 over the past 30 years, *Nat. Geosci.*, 2, 115–119,
963 <https://doi.org/10.1038/ngeo414>, 2009.
964
965 Wang, H., Easter, R. C., Rasch, P. J., Wang, M., Liu, X., Ghan, S. J., Qian, Y., Yoon,
966 J.-H., Ma, P.-L., and Vinoj, V.: Sensitivity of remote aerosol distributions to
967 representation of cloud–aerosol interactions in a global climate model, *Geosci.*
968 *Model Dev.*, 6, 765–782, <https://doi.org/10.5194/gmd-6-765-2013>, 2013.
969
970 Wang, H., Rasch, P. J., Easter, R. C., Singh, B., Zhang, R., Ma, P.-L., Qian, Y.,
971 Ghan, S. J., and Beagley, N.: Using an explicit emission tagging method in
972 global modeling of source-receptor relationships for black carbon in the Arctic:
973 Variations, sources, and transport pathways, *J. Geophys. Res.-Atmos.*, 119,
974 12888–12909, <https://doi.org/10.1002/2014JD022297>, 2014.
975
976 Wild, M.: Global dimming and brightening: A review, *J. Geophys. Res.*, 114,
977 D00D16, <https://doi.org/10.1029/2008JD011470>, 2009.
978

979 Yang, Y., Wang, H., Smith, S. J., Ma, P.-L., and Rasch, P. J.: Source attribution of
 980 black carbon and its direct radiative forcing in China, *Atmos. Chem. Phys.*, 17,
 981 4319-4336, <https://doi.org/10.5194/acp-17-4319-2017>, 2017a.
 982
 983 Yang, Y., Wang, H., Smith, S. J., Easter, R., Ma, P.-L., Qian, Y., Yu, H., Li, C., and
 984 Rasch, P. J.: Global source attribution of sulfate concentration and direct and
 985 indirect radiative forcing, *Atmos. Chem. Phys.*, 17, 8903-8922,
 986 <https://doi.org/10.5194/acp-17-8903-2017>, 2017b.
 987
 988 Yang, Y., Wang, H., Smith, S. J., Zhang, R., Lou, S., Yu, H., Li, C., and Rasch, P. J.:
 989 Source apportionments of aerosols and their direct radiative forcing and long-
 990 term trends over continental United States, *Earth's Future*, 6, 793–808,
 991 <https://doi.org/10.1029/2018EF000859>, 2018a.
 992
 993 Yang, Y., Wang, H., Smith, S. J., Zhang, R., Lou, S., Qian, Y., Ma, P.-L., and Rasch,
 994 P. J.: Recent intensification of winter haze in China linked to foreign emissions
 995 and meteorology, *Sci. Rep.*, 8, 2107, [https://doi.org/10.1038/s41598-018-20437-](https://doi.org/10.1038/s41598-018-20437-7)
 996 7, 2018b.
 997
 998 Yang, Y., Smith, S. J., Wang, H., Lou, S., and Rasch, P. J.: Impact of anthropogenic
 999 emission injection height uncertainty on global sulfur dioxide and aerosol
 1000 distribution, *J. Geophys. Res.-Atmos.*, 124, 4812–4826.
 1001 <https://doi.org/10.1029/2018JD030001>, 2019.
 1002
 1003 Zhang, Q., Jiang, X., Tong, D., Davis, S. J., Zhao, H., Geng, G., Feng, T., Zheng, B.,
 1004 Lu, Z., Streets, D. G., Ni, R., Brauer, M., van Donkelaar, A., Martin, R. V., Huo,
 1005 H., Liu, Z., Pan, D., Kan, H., Yan, Y., Lin, J., He, K., and Guan, D.:
 1006 Transboundary health impacts of transported global air pollution and
 1007 international trade, *Nature*, 543, 705–709, <https://doi.org/10.1038/nature21712>,
 1008 2017.
 1009
 1010
 1011

Table 1. Annual emissions (Tg yr⁻¹), concentrations (µg m⁻³), column burden (mg m⁻²), AOD (scaled up by a factor of 100) and DRF (W m⁻²) of Sulfate, BC, POA, SBP (sulfate-BC-POA) and [SBP-SOA](#) (sulfate-BC-POA-SOA) in Europe averaged over 1980–1984 and 2014–2018, as well as the differences between 1980–1984 and 2014–2018. Differences in percentage relative to mean values in 1980–1984 are presented in parentheses.

		Emis.	Conc.	Burden	AOD*100	DRF
Sulfate	1980–1984	15.10	6.00	14.35	9.13	-3.27
	2014–2018	2.53	1.80	5.79	3.24	-1.24
	Δ	-12.57 (-83.2)	-4.20 (-70.0)	-8.55 (-59.6)	-5.89 (-64.6)	2.04 (-62.2)
BC	1980–1984	0.47	0.4	0.38	0.7	--
	2014–2018	0.25	0.23	0.28	0.5	--
	Δ	-0.22 (-45.8)	-0.17 (-43.0)	-0.11 (-27.6)	-0.21 (-29.2)	--
POA	1980–1984	1.24	1.12	1.12	0.63	--
	2014–2018	0.94	0.86	1.08	0.58	--
	Δ	-0.30 (-24.4)	-0.26 (-23.2)	-0.04 (-3.8)	-0.05 (-7.5)	--
Sulfate-BC-POA	1980–1984	--	7.52	15.85	10.46	--
	2014–2018	--	2.89	7.15	4.32	--
	Δ	--	-4.63 (-61.6)	-8.70 (-54.9)	-6.15 (-58.7)	--
SBP-SOA	1980–1984	--	10.48	19.58	11.92	--
	2014–2018	--	4.34	8.55	5.44	--
	Δ	--	-6.14 (-58.6)	-11.03 (-56.3)	-6.48 (-54.37)	--

Deleted: PM_{2.5}

Deleted: PM_{2.5}

1023 **Table 2.** Relative contributions (%) of emissions from major source regions to the
1024 changes in near-surface concentrations, column burden, AOD and DRF in Europe
1025 between 1980–1984 and 2014–2018.
1026

	Sulfate-BC- POA			
	Δ Conc.	Δ Burden	Δ AOD	
EUR	92.8	91.2	91.2	
NAM	1.8	10.0	6.5	
NAF	-1.0	-1.5	-1.6	
MDE	-0.9	-1.9	-1.5	
EAS	-0.3	-3.1	-1.7	
RBU	8.0	9.2	8.5	
OTH	-0.1	-4.2	-2.0	
OCN	-0.3	0.2	0.6	
	Sulfate			
	Δ Conc.	Δ Burden	Δ AOD	Δ DRF
EUR	91.3	89.2	88.9	88.2
NAM	2.1	10.5	6.9	
NAF	-0.6	-0.9	-0.8	
MDE	-0.8	-1.7	-1.3	
EAS	-0.3	-2.8	-1.4	
RBU	8.6	9.5	8.7	
OTH	-0.1	-4.0	-1.8	
OCN	-0.3	0.3	0.7	

1027
1028
1029

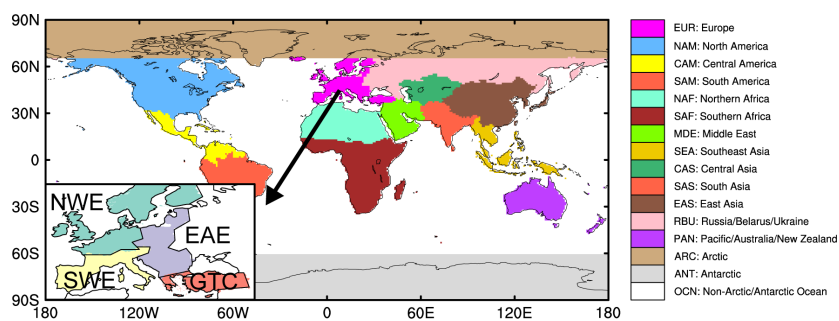
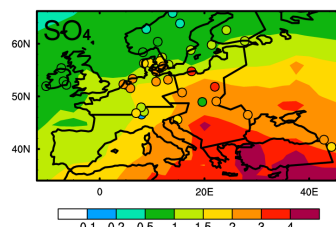
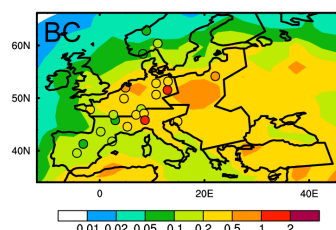


Figure 1. Source regions that are selected for the Explicit Aerosol Source Tagging (EAST) in this study, including Europe (EUR), North America (NAM), Central America (CAM), South America (SAM), North Africa (NAF), South Africa (SAF), the Middle East (MDE), Southeast Asia (SEA), Central Asia (CAS), South Asia (SAS), East Asia (EAS), Russia-Belarus-Ukraine (RBU), Pacific-Australia-New Zealand (PAN), the Arctic (ARC), Antarctic (ANT), and Non-Arctic/Antarctic Ocean (OCN). The embedded panel (at bottom left) is Europe, as the receptor region, which is further divided to Northwestern Europe (NWE), Southwestern Europe (SWE), Eastern Europe (EAE) and Greece-Turkey-Cyprus (GTC).

a NMB = -14% R = 0.62



b NMB = -13% R = 0.43



c NMB = -23% R = 0.57

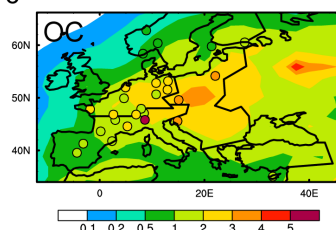
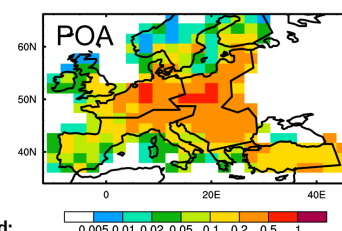
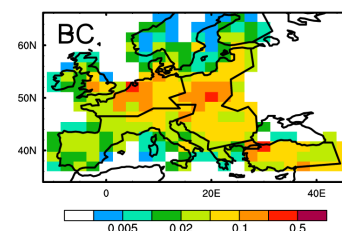
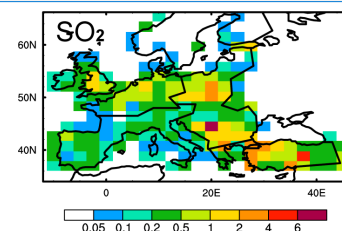
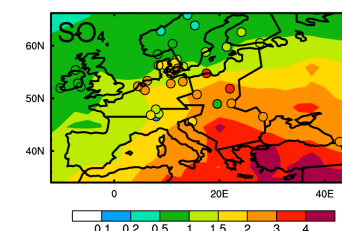


Figure 2. Spatial distribution of simulated (contour) and observed (color-filled circles) annual mean near-surface (a) sulfate, (b) BC, and (c) OC (derived as (POA+SOA)/1.4 in model) concentrations ($\mu\text{g m}^{-3}$) over 2010–2014. Observations are from EMEP (European Monitoring and Evaluation Programme) networks. Normalized mean bias (NMB = $100\% \times \sum (Model_{site} - Observation_{site}) / \sum Observation_{site}$) and correlation coefficient (R) between observed and simulated concentrations are noted at the top of each panel.

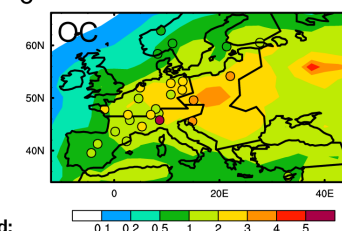


Deleted: ... [1]

a NMB = -14% R = 0.62



c NMB = -23% R = 0.57



Deleted: ... [2]

Deleted: 3.... Spatial distribution of simulated (contour) and observed (color-filled circles) annual mean near-surface (a) sulfate, (b) BC, and (c) OC (derived as (POA+SOA)/1.4 in model) and (d) PM_{2.5} (sulfate+BC+POA+SOA in model)

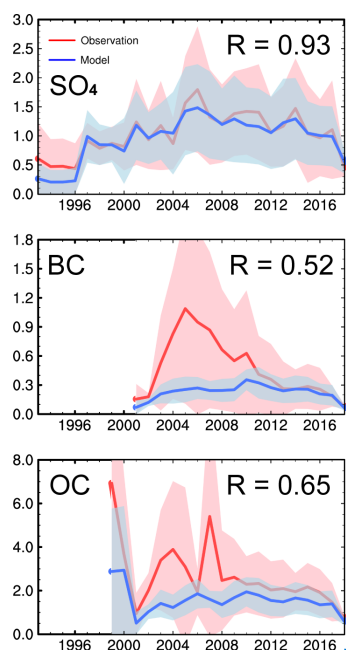
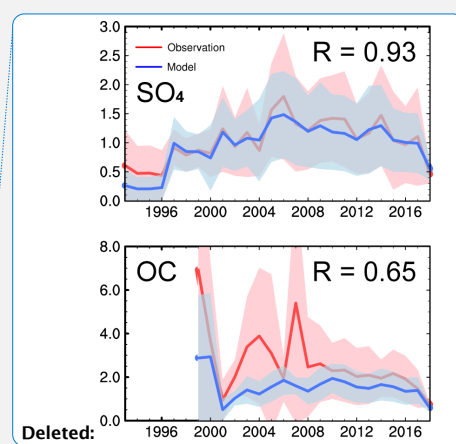


Figure 3. Time series (1993–2018) of spatial and annual mean near-surface (a) sulfate, (b) BC, and (c) OC concentrations ($\mu\text{g m}^{-3}$) in Europe from model simulation (blue lines) and observations (red lines). Model results are plotted only when EMEP observational data are available. Shaded areas represent 1- σ spatial standard deviation of annual mean concentrations for each year. Temporal correlation coefficients (R) between observed and simulated spatially averaged concentrations are noted on the top-right corner of each panel.



Deleted: 4

Deleted: and PM_{2.5}

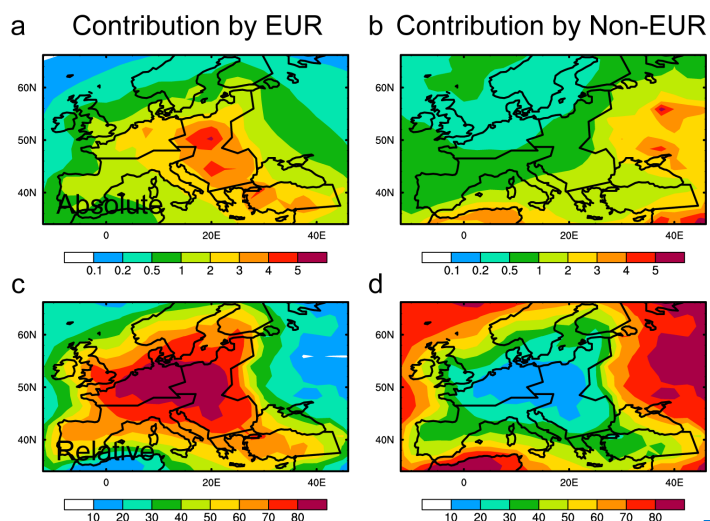
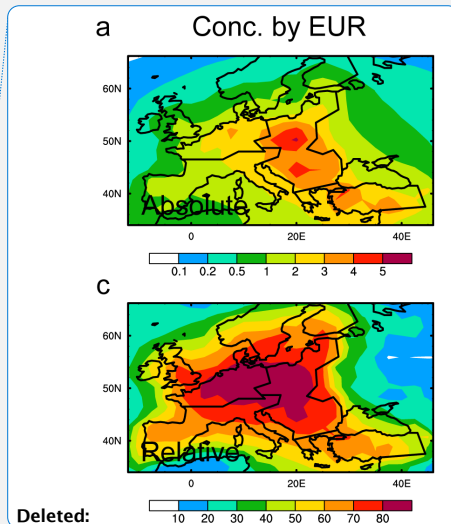


Figure 4. (a,b) Absolute ($\mu\text{g m}^{-3}$) and (c,d) relative contributions (%) to annual mean near-surface concentrations of sulfate-BC-POA from European local emissions (EUR) and emissions outside the Europe (Non-EUR), respectively, averaged over 2010–2018.



Deleted:

Deleted: 5

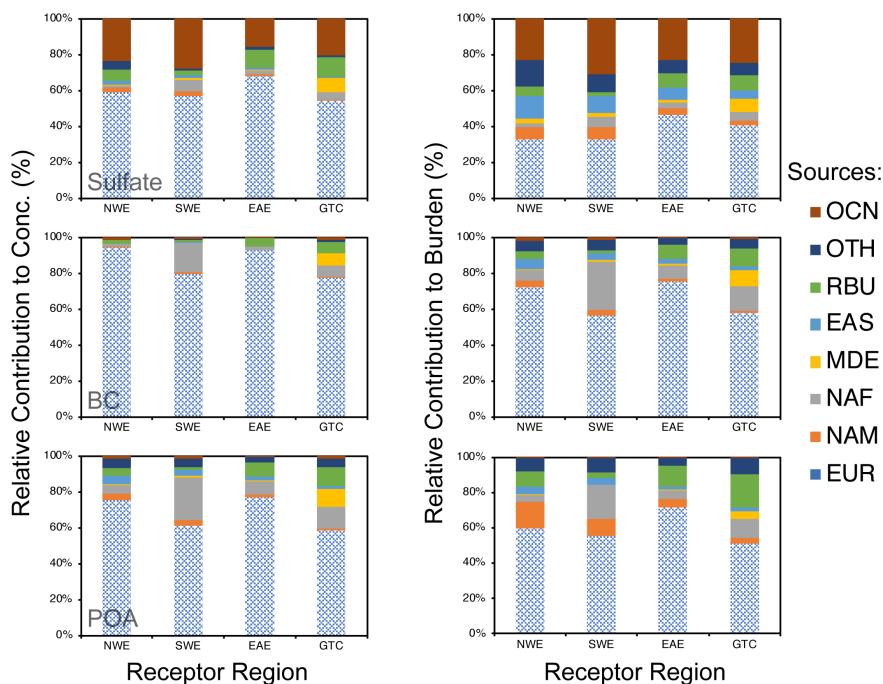


Figure 5. Relative contributions (%) by emissions from major tagged source regions including Europe (EUR), North America (NAM), North Africa (NAF), the Middle East (MDE), East Asia (EAS), Russia-Belarus-Ukraine (RBU), Non-Arctic/Antarctic Ocean (OCN) and other (OTH) regions, to near-surface concentrations (left) and column burdens (right) of sulfate, BC and POA (from top to bottom) in the four sub-regions of Europe averaged over 2010–2018. Patterned areas represent EUR local contributions.

- Deleted: 6
- Deleted: (
- Deleted: EUR, NAM
- Deleted: NAF
- Deleted: MDE
- Deleted: EAS
- Deleted: RBU
- Deleted: OCN)
- Deleted: (OTH=CAM+SAM+SAF+SEA+CAS+SAS+PAN+ARC+ANT)...
- Deleted: ¶

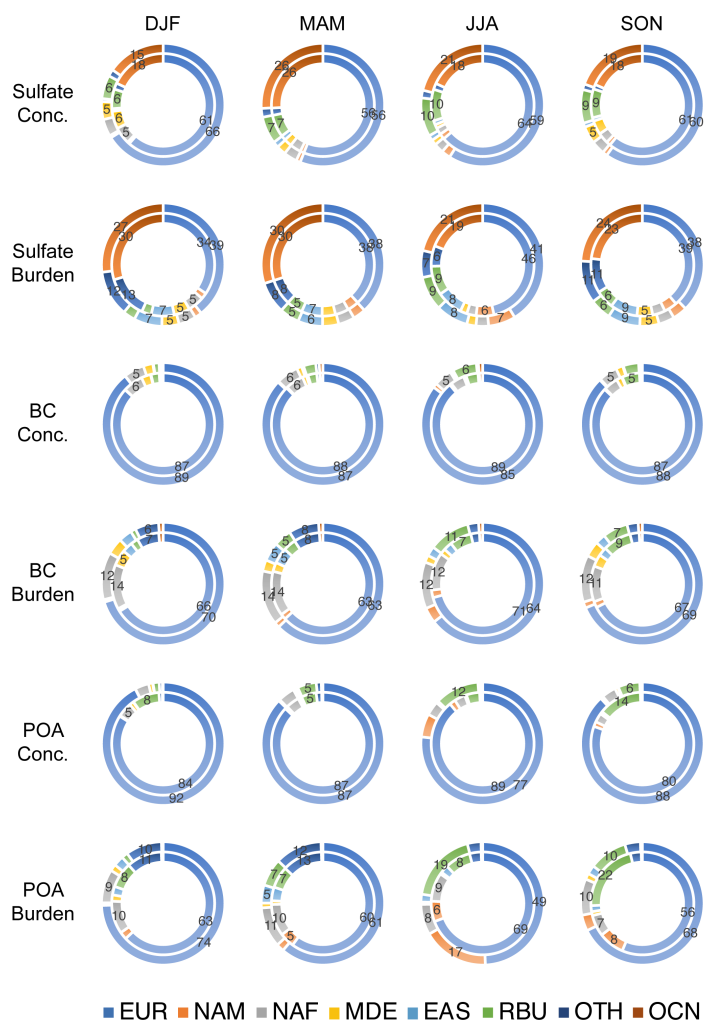


Figure 6. Relative contributions (%) by emissions from major tagged source regions to near-surface concentrations (Conc.) and column burdens of December-January-February (DJF), March-April-May (MAM), June-July-August (JJA) and September-October-November (SON) mean sulfate, BC and POA over the Europe averaged over 2010–2018. Outer rings represent the modeled values and the relative contributions in inner rings is calculated based on absolute values normalized by the ratio of seasonal emission to annual mean. Values larger than 5% are marked.

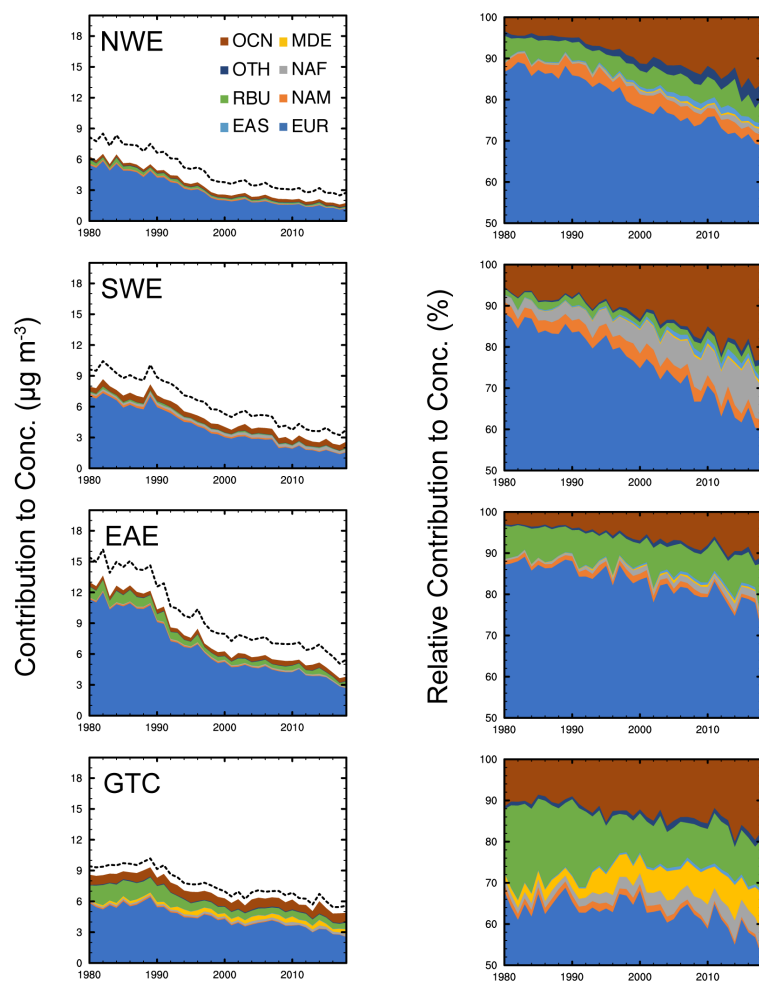


Figure 7. Time series (1980–2018) of absolute (left, $\mu\text{g m}^{-3}$) and relative (right, %) contributions of emissions from major source regions to the simulated annual mean near-surface sulfate-BC-POA concentrations averaged over the four sub-regions of Europe. Dashed lines in left panels represent simulated aerosol concentrations including SOA.

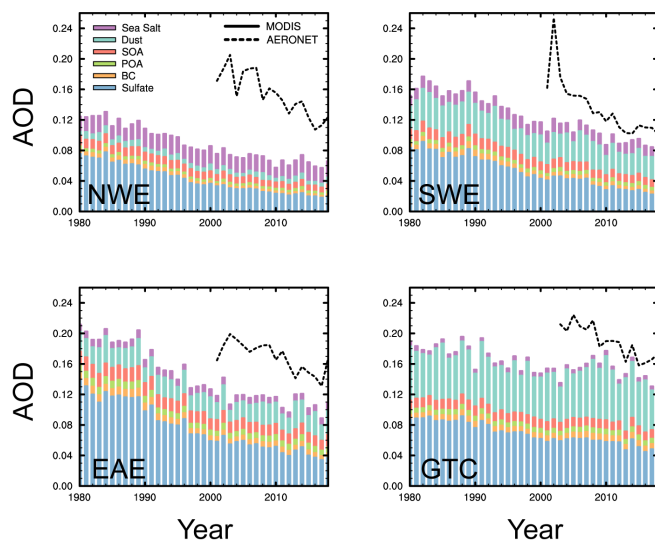


Figure 8. Time series (1980–2018) of simulated annual mean AOD for sulfate, BC, POA, SOA, dust and sea salt averaged over the four sub-regions of Europe. Dashed lines represent AOD from AERONET measurements.

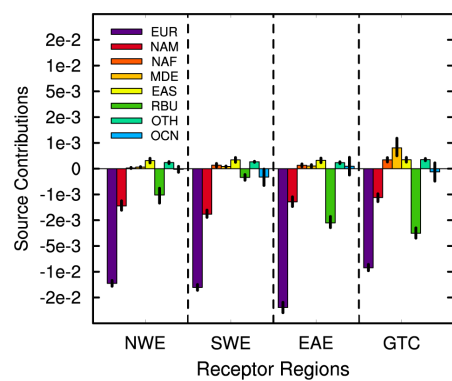


Figure 9. Absolute contributions (decade⁻¹) of the emissions from major source regions to the trends of sulfate AOD over the four sub-regions of Europe. Error bars represent 95% confidence intervals of the linear regression.

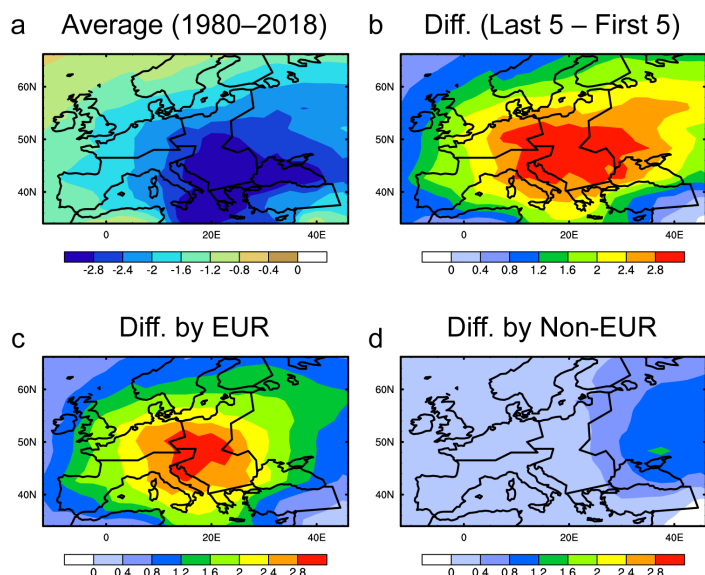


Figure 10. (a) Simulated annual mean DRF (W m⁻²) of sulfate averaged over 1980–2018 and (b) the difference in sulfate DRF between 1980–1984 and 2014–2018. The contributions of European and non-European emissions to the difference are given in (c) and (d), respectively.

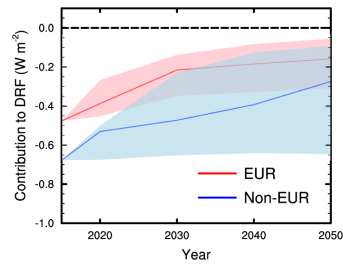


Figure 11. Time series (2015–2050) of estimated annual mean sulfate DRF over Europe contributed by European and non-European emissions. Lines and areas represent median values and minimum-to-maximum ranges of the estimated sulfate DRF from eight SSP scenarios, including SSP1-1.9, SSP1-2.6, SSP2-4.5, SSP3-7.0, SSP4-3.4, SSP4-6.0, SSP5-3.4, and SSP5-8.5. Future DRF of sulfate aerosol over Europe is estimated by scaling historical mean (1980–2018) sulfate DRF using the ratio of SSPs future SO₂ emissions to historical emissions assuming a linear response of DRF to regional emissions.

Page 41: [1] Deleted	Yang Yang	12/17/19 10:16:00 PM
----------------------	-----------	----------------------

Page 41: [2] Deleted	Yang Yang	12/17/19 10:16:00 PM
----------------------	-----------	----------------------

Page 41: [2] Deleted	Yang Yang	12/17/19 10:16:00 PM
----------------------	-----------	----------------------